ELSEVIER

PII: S0032-3861(97)10109-4

Polymer Vol. 39 No. 25, pp. 6347–6355, 1998

0032-3861/98/$ - see front matter

The Torsional Impedance test: short-time, large-strain stress response in tough polymers

S. J. K. Ritchie* and P. S. Leevers
Department of Mechanical Engineering, Imperial College, London SW7 2BX, UK
(Received 30 June 1997; accepted 4 September 1997)

Tough polymers (especially crystalline polyolefins) tend to show brittle behaviour, with a pronounced drop in fracture toughness, at high crack speeds. Since this effect is of special industrial importance, the High Speed Double Torsion test has been developed to measure it. Extracting fracture resistance data from the test demands accurate dynamical stress analysis of the specimen, but bulk strains are usually large enough to induce pronounced stress–strain non-linearity. The Torsional Impedance test was devised to acquire shear stress–strain data for corresponding geometries and loading times. The original analysis is here shown to have been flawed and it is corrected according to a more complete model, implemented as a numerical finite-difference scheme. Data are presented for modified high density polyethylene, and for pure and rubber-toughened grades of both polyoxymethylene and polypropylene. © 1998 Elsevier Science Ltd. All rights reserved.

(Keywords: dynamic; non-linear; finite-difference)

INTRODUCTION

The development of the Torsional Impedance test was motivated by the need to quantify non-linear-elastic material properties observed in the High Speed Double Torsion (HSDT) test. The HSDT test is a high rate version of the standard double torsion fracture test. It was developed by Leevers[1] to induce steady rapid crack propagation (RCP) in tough polymers. The experimental results are used to determine a material's dynamic fracture resistance (G_D) as a function of crack velocity. The HSDT test specimen, a plate 100 mm by 200 mm and 10 mm thick, rests horizontally on four radiused support points. As shown in *Figure 1*, a fast-moving striker, carrying two similarly radiused points, hits the specimen from above between the two support points near one end. Continuing at almost constant speed (typically 5–35 m/s), the striker initiates a crack (usually from an initial notch) and drives it along the specimen centreline at controlled speed (typically 50–350 m/s) by applying equal and opposite torsion. The reaction force and the crack length are recorded continuously.

The specimen is analysed as two rectangular-sectioned torsion beams, lying side by side but joined only beyond the crack tip. As the crack approaches, each beam section starts to rotate, accelerating until the crack has passed; after which rotation continues at a more constant rate. Because deformation is symmetric about the crack plane, the 'beam rotation profile' $\theta(z)$ (*Figure 1*) provides a complete description of bulk specimen deformation. The torsion or twist $\partial\theta/\partial z$ largely determines local strains, and $\partial^2\theta/\partial z^2$ largely determines strain rates. Broadly speaking, each section suffers a short period of rapid loading, during which it communicates some energy to the passing crack front, followed by a longer period under almost constant deformation at high strain.

In order to determine G_D from the HSDT experimental results a post-mortem analysis must be performed. The analysis must model the deformation during the test so that the work done by the striker can be partitioned into strain, kinetic and fracture energies as a function of time[2]. Wheel has developed the most advanced analysis of the test to date. It is based on numerically integrating a one (spatial) dimensional torsional wave equation using the finite difference (FD) method. His equation was based on Gere's[3], which included the effects of axial stresses but not axial inertia.

The value of G_D calculated from the HSDT analysis is strongly dependent on the secant and tangent shear moduli. These moduli, together with the section geometry and boundary conditions, control the amplitude and velocity of torsional waves. Wheel's[2] initial analysis of the HSDT test specimen used a linear-elastic material model. He used a direct contact ultrasonic technique developed by Dioh[4] to determine both the tensile (E) and shear (μ_0) moduli. These moduli correspond to a low strain (0.1%) and a high strain rate (20 000 s^{-1}). His model over-predicted the experimental load by approximately 25%, the disparity varying little with strain. The over prediction led him to the conclusion that, even during this short loading time, the shear modulus decreased with increasing strain.

To acquire quantitative non-linear material property data, Wheel developed a Torsional Impedance test[5]. The test consists of measuring the impedance of the rectangular beams to an imposed rotation rate. To achieve this an unmodified HSDT test rig is used. The sample consists of a pre-fractured HSDT specimen which is re-assembled and loosely held together at the end furthest from the load point. Although visco-elastic strain rate effects are not directly accounted for, the rates in the Torsional Impedance test are similar to those produced in the HSDT test.

Wheel proposed a definition of effective strain which was proportional to striker velocity. He calculated the associated effective shear modulus from the load. He demonstrated that the shear modulus did indeed reduce with strain, and included the measured non-linear properties in his analysis of the HSDT test. The non-linear analysis further reduced

* To whom correspondence should be addressed

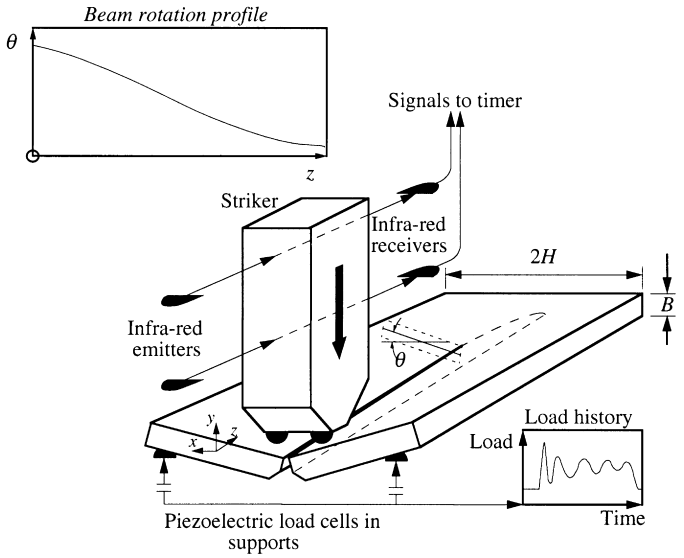

Figure 1 Schematic of the high speed double torsion test

the scatter in G_D results and reduced the disparity between predicted and experimental load.

A FINITE DIFFERENCE MODEL OF THE TORSIONAL IMPEDANCE TEST

Before examining the Torsional Impedance test further, a model of it is introduced. This model is subsequently used to validate assumptions made in deriving a simplified, analytical solution for the test specimen deformation.

Wheel's FD model of the HSDT test can easily be adapted to model the Torsional Impedance test, which is merely an HSDT test on a zero-G_D material. However, a new, more accurate, fourth-order, partial differential equation governing torsion of rectangular bars was given in Ref. 6. The equation was derived from two second-order equations whereby an axial displacement variable was eliminated. A new FD program was written to integrate simultaneously the non-dimensional forms of the two second-order equations. An explicit, second-order accurate, central difference scheme was used. This was shown to be both efficient and stable by Wheel[2]. To ensure stability, the time step must be less than the time taken for a disturbance, travelling at the maximum possible velocity, to traverse the distance between two adjacent nodes. The time step chosen was one fifth of the time it takes a shear wave (asymptotic phase velocity of dispersive torsional waves at high frequencies) to travel between two adjacent nodes. A nodal spacing of 1.667 mm was found to ensure convergence.

Resonance test case

The analytical solution of the equation for torsional resonance of rectangular section beams was given in [6]. This was used as a test case for the FD model: initial nodal rotations and axial displacements were set to correspond to a specific resonance mode. The model was then used to predict the resulting deformation. The model geometry corresponded to the standard HSDT half-specimen and the linear-elastic material properties were used. The predicted frequency of oscillation was within 0.01% of that calculated analytically and the mode shape showed no change over 20 oscillations. This procedure was repeated for all mode numbers up to the 16th, with no increase in the discrepancy between analytical and FD results.

Boundary conditions

The boundary conditions for the Torsional Impedance test model are the same as those used to model the low rate DT test in Ref. 7.

The load trace from a Torsional Impedance test shows characteristic oscillations about a mean load. Work by Williams[9] and Crouch[10] on the three-point-bend specimen showed that two possible causes for the oscillation are contact stiffness and overhang (the region between the load point and free end) effects. The modelling of the overhang is already included in the FD model as described in Ref. 7.

The contact stiffness between the spherical contact points and the planar specimen surface was included in the model via the solution of Hertz[11]. His solution assumes linear elasticity and zero friction or relative slip between the contacting surfaces:

$$\alpha = \left(\frac{9}{16} \frac{\pi^2 (c_1 + c_2)^2}{R} \right)^{\frac{1}{3}} P^{2/3}$$

where α is the distance that the two bodies approach one another after contact, P is the contact force and R is the radius of the contact point. $c_n = (1 - \upsilon_n^2)/(\pi E_n)$ is a compliance term, the subscript $n = 1$ or 2 denoting the different material properties of the two bodies, E being the tensile modulus and υ the Poisson's ratio. The value assigned to E for the specimen is the product of μ_0 and an adjustment factor (χ). The adjustment factor was introduced since the value of E appropriate to the strain and strain rate at the contact point is unknown prior to performing the analysis. The value of χ is calculated by matching the oscillation amplitude of the experimental and predicted load histories.

The load–plane rotation (θ_L) in the Torsional Impedance test can approach 30°. Leevers and Williams[8] gave a large displacement correction:

$$\chi = D \tan \theta_L - \kappa(\sec \theta_L - 1),$$

which can be inverted to give:

$$\theta_L = \arcsin\left(\frac{\kappa}{\sqrt{D^2 + (\kappa - \nu)^2}} \right) - \arctan\left(\frac{\kappa - \nu}{D} \right)$$

where ν is striker displacement, D is the distance between

the support and load points, and $\kappa = R_1 + R_2 + B$ where R_1, R_2 are the radii of the support and load points and B is the specimen thickness. The value of ν is equal to the difference between the striker displacement and the sum of α at the support and load points.

The above equations governing θ_L, together with boundary conditions for the specimen itself at this plane, are solved in the FD model at each step. Deceleration of the striker due to the reaction load is also accounted for.

THE TORSIONAL IMPEDANCE TEST ANALYSIS

In theory, the FD model described above could be used to determine the dependence of the effective shear moduli on effective strain. In practice this is extremely difficult since there is a large variation in strain along the specimen. Since only two parameters are measured during a test (load and striker velocity) a wide range of stress–strain curves could be used to match FD predictions to any one test. An iterative process would therefore be required, performing the test at a range of striker speeds, analysing each test with a first guess stress–strain curve and then adjusting the model on comparing the FD and experimental results. A simplified analytical analysis is therefore required which can be used to derive a non-linear stress–strain curve directly from the experimental results.

Review

A typical load trace (*Figure 2*) shows, after an initial peak, an oscillation about a constant mean value. The mean load increases with striker velocity. The nature of the oscillation is largely determined by the overhang region behind the load plane: this can be demonstrated by comparing the contact load predicted using the FD model with and without the overhang. These results are also shown in *Figure 2*.

Figure 3 shows an instantaneous beam rotation profile predicted from the finite difference solution during the constant load period. The region in front of the load plane region is subjected to uniform torsion (constant twist). This is expected since a constant rotation rate is applied and any local variations in the twist would quickly disperse.

The wave speed in this region must therefore equal that predicted from the torsional equation of motion for uniform torsion[6] (which is identical to Saint-Venant's solution):

$$C_t = \sqrt{\frac{\lambda \mu_t}{\rho}}$$

where ρ is the density, λ is a section constant and μ_t is the effective section tangent shear modulus as defined in [6]. Wheel assumed that $\mu_t = \mu_0$, the low strain, high strain rate shear modulus. Knowing the section rotation rate

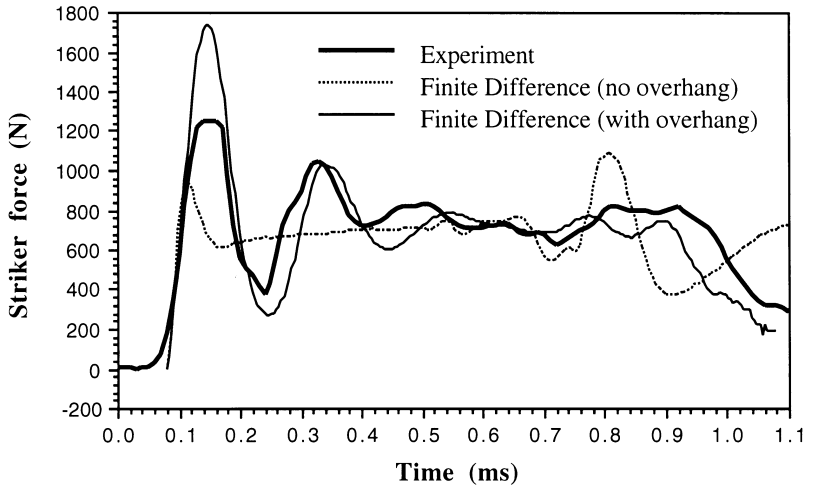

Figure 2 Experimental and predicted load traces (HDPE, 0°C, striker velocity = 22.2 m/s)

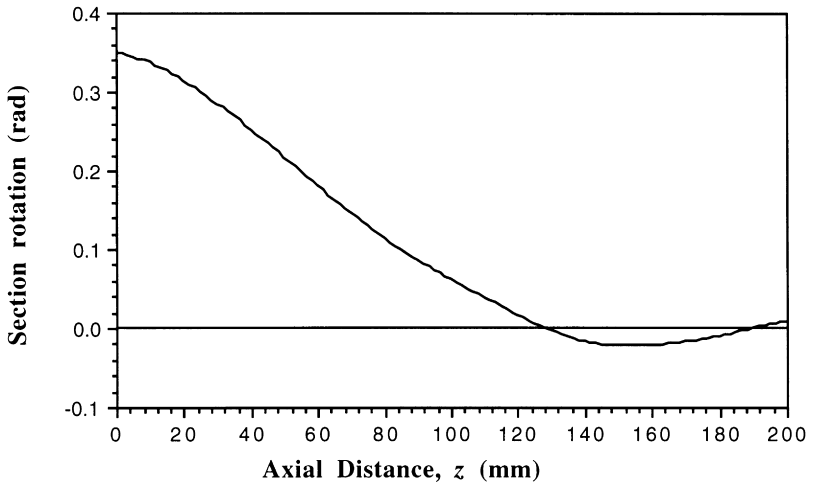

Figure 3 Predicted beam rotation profile during Torsional Impedance test (HDPE, 0°C, striker velocity = 22.2 m/s)

imposed by the striker ($\dot{\theta}_L$) he calculated the twist in the deformed region as:

$$\left(\frac{\partial\theta}{\partial z}\right)_{\mathrm{L}} = \frac{\dot{\theta}_{\mathrm{L}}}{C_{\mathrm{t}}^0} \tag{1}$$

where C_{t}^0 is the Saint-Venant torsional wave speed calculated assuming $\mu_{\mathrm{t}} = \mu_0$. Wheel then defined an effective strain (γ_{e}) equal to $B(\partial\theta/\partial z)$ the maximum shear strain in the section. From equation (1) he was therefore able to calculate an effective strain from the striker speed.

The transmitted torque for the case of uniform torsion is given by Ritchie and Leevers[6] as:

$$T = \mu_{\mathrm{s}}\lambda J\frac{\partial\theta}{\partial z} \tag{2}$$

where J is the second moment of area of the section and μ_{s} is the effective secant shear modulus as defined in Ritchie and Leevers[6].

Wheel calculated the value of μ_{s} associated with the effective strain by substituting the experimentally measured mean torque and calculated twist into equation (2). By repeating the test at different striker velocities, he built up a definition for $\mu_{\mathrm{s}}(\gamma_{\mathrm{e}})$ and thereby calculated the effective tangent shear modulus in the normal manner:

$$\mu_{\mathrm{t}} = \frac{\partial}{\partial\gamma_{\mathrm{e}}}(\mu_{\mathrm{s}}\gamma_{\mathrm{e}}).$$

A revised analysis of the Torsional Impedance test

For a non-linear elastic material the wave speed at any point will be a function of the local tangent shear modulus (μ_{t}) which will depend on strain. By neglecting this dependence in assuming $\mu_{\mathrm{t}} = \mu_0$ to derive equation (3), Wheel under-predicted the strains and over-predicted the decay rate of μ_{s} with strain. Correcting the analysis means the twist can no longer be determined explicitly, since it depends on the value of μ_{t} which is to be calculated.

A more rigorous definition of γ_{e} was proposed in Ritchie and Leevers[6]. From γ_{e} an effective stress is defined as usual from Hooke's law as:

$$\tau_{\mathrm{e}} = \mu_{\mathrm{s}}\gamma_{\mathrm{e}}$$

where the effective strain, $\gamma_{\mathrm{e}} = (\lambda J/\Gamma_{\mathrm{c}})/(\partial\theta/\partial z)$ and for a rectangular section $\Gamma_{\mathrm{c}} = \frac{1}{4}BH(B+H)$

The effective stress is easily calculated from the experimental mean torque (equation (2)) as:

$$\tau_{\mathrm{e}} = \frac{T}{\Gamma_{\mathrm{c}}}$$

Substituting Wheel's evaluation for twist into the new definition of effective strain, but without making any assumption about μ_{t}, gives:

$$\frac{\mathrm{d}\tau_{\mathrm{e}}}{\mathrm{d}\gamma_{\mathrm{e}}} = \frac{1}{\mu_0}\left(\frac{\tau_0}{\gamma_{\mathrm{e}}}\right)^2 \tag{3}$$

where

$$\tau_0 = \frac{\mu_0\lambda J}{\Gamma_{\mathrm{c}}}\frac{\dot{\theta}_{\mathrm{L}}}{C_{\mathrm{t}}^0}$$

The variable τ_0 is the effective stress that would result if $\mu_{\mathrm{s}} = \mu_0$. The experimental results can now be used to define $\tau_{\mathrm{e}}(\tau_0)$ which should be independent of section dimensions. By the chain rule,

$$\frac{\mathrm{d}\tau_{\mathrm{e}}}{\mathrm{d}\gamma_{\mathrm{e}}} = \frac{\mathrm{d}\tau_{\mathrm{e}}}{\mathrm{d}\tau_0}\cdot\frac{\mathrm{d}\tau_0}{\mathrm{d}\gamma_{\mathrm{e}}}$$

Substituting from equation (3) and integrating by separation of variables, gives:

$$\frac{1}{\gamma_{\mathrm{e}}} = -\mu_0\int\left(\frac{\mathrm{d}\tau_{\mathrm{e}}/\mathrm{d}\tau_0}{\tau_0^2}\right)\mathrm{d}\tau_0 \tag{4}$$

Equation (4) thus allows the effective strain to be calculated as a function of effective stress.

Implementation of the analysis

In order to proceed with the evaluation of the shear moduli a mathematical form of $\tau_{\mathrm{e}}(\tau_0)$ must be specified. A typical set of normalised results from the Torsional Impedance test for an HDPE material is shown in *Figure 4*.

At first sight the data appear to lie on a straight line with a slope less than 1. This would imply both μ_{s} and μ_{t} to have strain independent values considerably less than μ_0. Results from section rotation measurements (see later) show that this cannot be true, since at low values of strain μ_{s} and μ_{t} are close to μ_0. The shear moduli must therefore approach μ_0 at low strains.

The approach taken here is to use a piece-wise linear fit to the experimental data $\tau_{\mathrm{e}}(\tau_0)$ defined as follows. Let $\tau_{\mathrm{e}}(\tau_0)$ be approximated by a consecutive series of N linear regions such that region n is defined by the two points, $n-1$ and n,

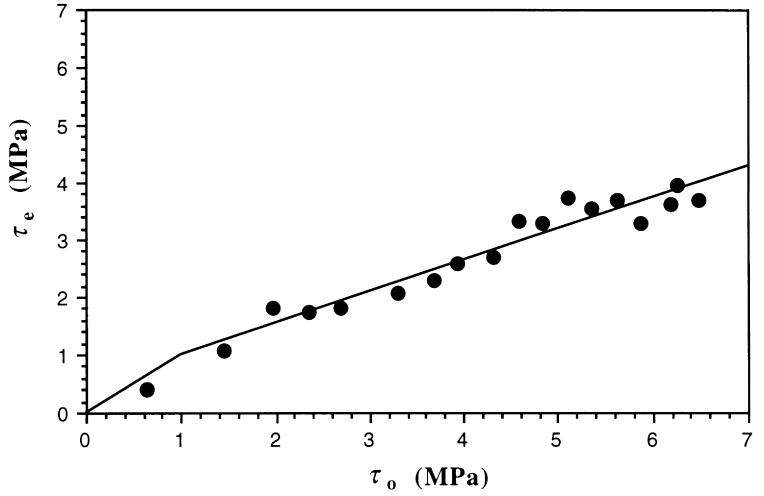

Figure 4 Torsional Impedance results for an HDPE

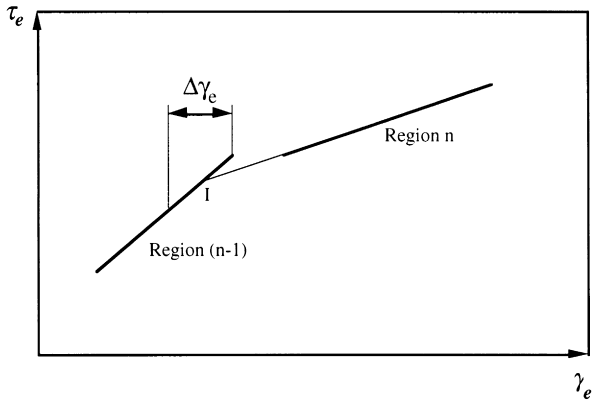

Figure 5 Schematic of effective stress–strain regions: $n-1$ and n

and is described by the following equation:

$$\tau_e = m_n(\tau_0 - \tau_0|_{n-1}) + \tau_e|_{n-1}$$

where the slope,

$$m_n = \frac{\tau_e|_n - \tau_e|_{n-1}}{\tau_0|_n - \tau_0|_{n-1}}$$

and

$$\tau_0|_{n-1} \leq \tau_0 \leq \tau_0|_n$$

Substituting into equation (4) and evaluating the integral gives the effective section secant and tangent moduli for region n as:

$$\mu_s = m_n^2\mu_0 + \frac{\tau_e|_{n-1} - m_n\tau_0|_{n-1}}{\gamma_e}$$

$$\mu_t = \mu_0 m_n^2$$

The strain which demarcates linear regions $n-1$ and n can take one of two values depending on which region is considered. Rather than using either of these two values the intercept is taken (point I in *Figure 5*):

$$\gamma_e|_{n-1} = \frac{\tau_0|_{n-1}}{\mu_0(m_{n-1} + m_n)}$$

The resulting stress–strain curve is also piece-wise linear; this produces numerical instability problems in the FD model due to the singularity in μ_t at intersections. Cubic spline fits between the linear regions are used to prevent this. Consider the spline connecting region $n-1$ and n. The mid strain of the spline is taken to correspond to the strain at the intercept (I). The interval of strain ($\Delta\gamma_e$) corresponding to the spline is taken to be twice the difference in strain between the intercept and strain defined by point $n-1$ of region $n-1$:

$$\Delta\gamma_e = 2\frac{\tau_0|_{n-1}}{\mu_0}\frac{m_n}{m_{n-1}(m_n + m_{n-1})}$$

VALIDATION

Finite difference model

The original experimental results were regenerated with the FD model, using the material stress–strain characteristic derived above. The results (*Figure 6*) show a slight reduction in τ_e. The error is probably due to assuming the load plane rotation rate to be constant, whereas it actually varies slightly through the test. This assumption could be modified, but on noting the scatter of the experimental results the apparent reduction in τ_e is relatively insignificant.

Section rotation

A powerful advantage of the DT geometry is that large out-of-plane deflections on the surface allow the use of an optical crack gauge[12]. A modified form of this gauge can be used to measure rotation at a series of sections along the specimen as a function of time. Comparing the section rotation measurements during a Torsional Impedance test to those predicted using the FD model allows the theory to be validated. The optical crack gauge was primarily designed to identify times at which angular acceleration occurs at a section, rather than to measure absolute rotation values; quantitative results for angular rotation show considerable scatter.

Software post-processing was used to determine the time at which each of the section rotations passed through a minimum (low strain) and reached 8° (high strain). A 'propagation rate' (V) of that rotation along the specimen was then evaluated. The corresponding propagation rate was then predicted using the FD model. The tests analysed correspond to those shown in *Figure 3*. There is good agreement between the FD model and experimental results

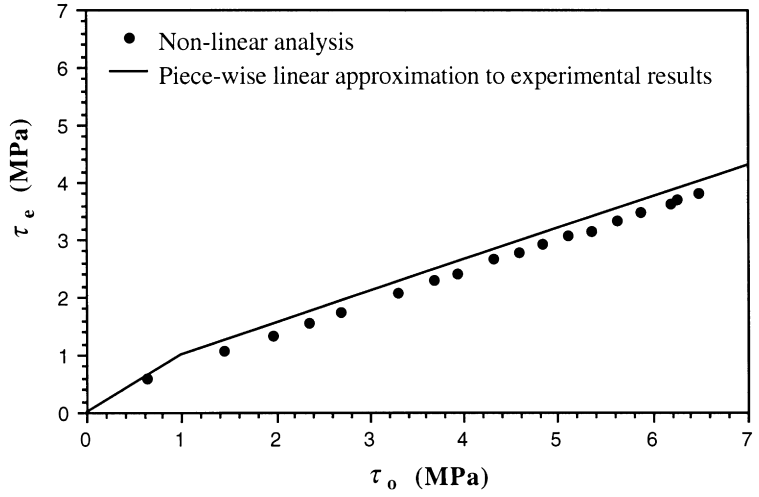

Figure 6 Normalised Torsional Impedance test results and the equivalent values predicted from the finite difference model

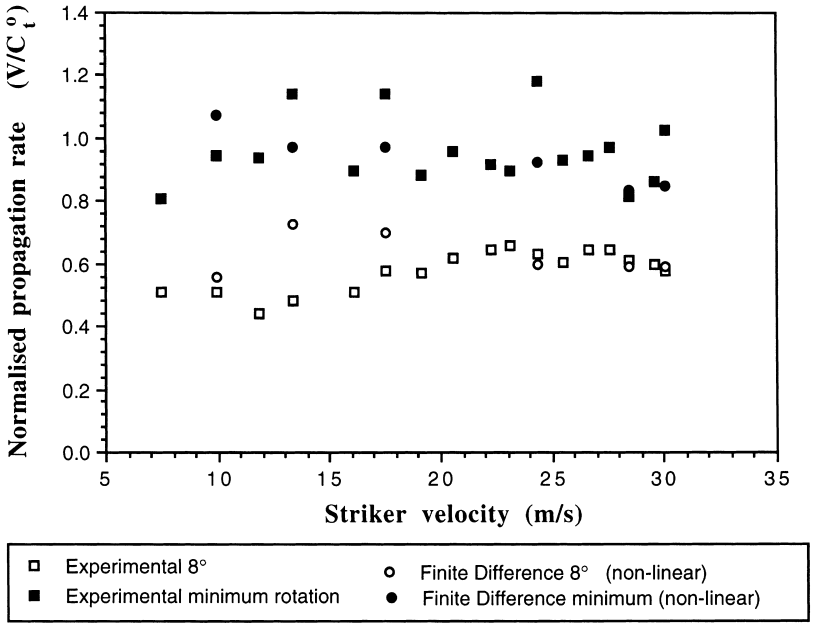

Figure 7 Experimental and predicted propagation rates of the minimum rotation amplitude

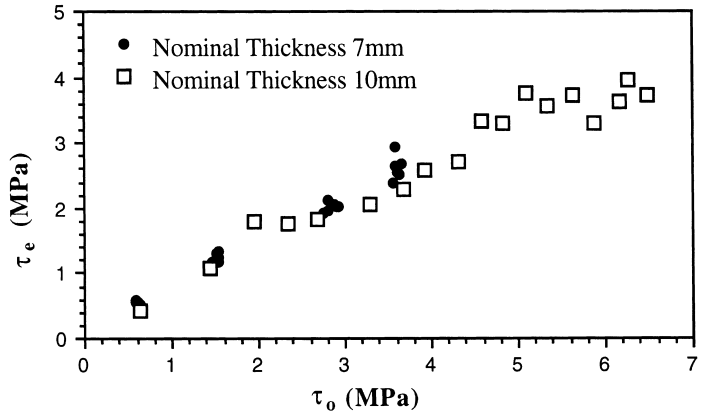

Figure 8 Torsional Impedance results for 7 and 10 mm thicknesses of HDPE at 0°C (7 mm results from Wheel[13])

(*Figure 7*). The propagation rate of the minimum rotation is, on average, just less than C_t^0 indicating that $\mu_s = \mu_t = \mu_0$ in this low-strain region.

Geometry dependence

Figure 8 shows Torsional Impedance test results for two thicknesses (7 and 10 mm) of the same grade of HDPE. The figure shows the results to be similar, despite the three-fold increase in section rigidity, and confirms that the effective section modulus is geometry independent.

RESULTS

Non-linear material results from the Torsional Impedance test

Torsional Impedance and ultrasonic modulus tests were performed on a range of materials. In each case the specimens were 10 mm thick, produced by compression moulding. All the results could be modelled adequately by a bilinear fit. They are summarised in *Table 1*.

For all the results apart from the pure polypropylene homopolymer the high strain shear modulus is considerably less than μ_0. For the HDPE at 0°C, the maximum section strain corresponding to the effective strain demarking the transition point between the two regions is approximately 0.8%. This corresponds approximately to a 1.6% normal strain (assuming pure shear stress conditions) which is close to the yield point of the material[14]. The transition may therefore be due to the onset of the section yielding. As the effective section shear strain increases beyond the transition a larger and larger proportion of the section undergoes yielding. This effect manifests itself as a reduction in the effective section shear modulus which remains constant after the initial transition period.

Oscillations in the load trace

The present work on the FD model has led to a much deeper understanding of the characteristic oscillations seen in the load. There are a number of aspects to these oscillations which are discussed separately below.

The main cause of the oscillations is not the contact stiffness but the overhang region behind the contact point, as demonstrated in *Figure 2*. Torsional Impedance tests were performed on HDPE at −5°C with two different overhang lengths of 5 and 15 mm. The load histories for each test were recorded and compared with those predicted by the FD

Table 1 Summary of Torsional Impedance test results

Material		High density polyethylene	Polyoxymethylene (unmodified)	Polyoxymethylene (toughened)	Polypropylene (unmodified)	Polypropylene (toughened)
Temperature (°C)		0	0	0	0	0
μ_0 (GPa)		1.127	1.783	1.209	1.79	0.856
Poisson's ratio (υ)		0.38	0.37	0.38	0.33	0.40
Density (kg/m^3)		960	1420	1330	912.3	894.9
Slope (m_1)		0.544	0.545	0.394	0.951	0.844
Point 1	τ_0 (MPa)	1.047	0.706	0.172	0.0	0.593
	τ_e (MPa)	1.047	0.706	0.172	0.0	0.593
Point 2	τ_0 (MPa)	7.00	10.00	8.00	6.0	5.00
	τ_e (MPa)	4.29	5.77	3.26	5.706	4.31
$(m_1)^2\mu_0$ (GPa)		0.33	0.53	0.19	1.61	0.61

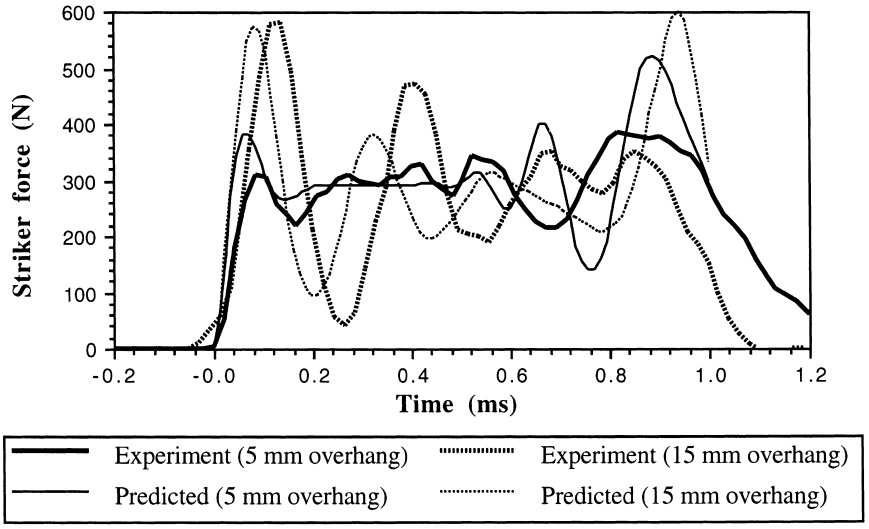

Figure 9 Dependence of load oscillations on overhang length

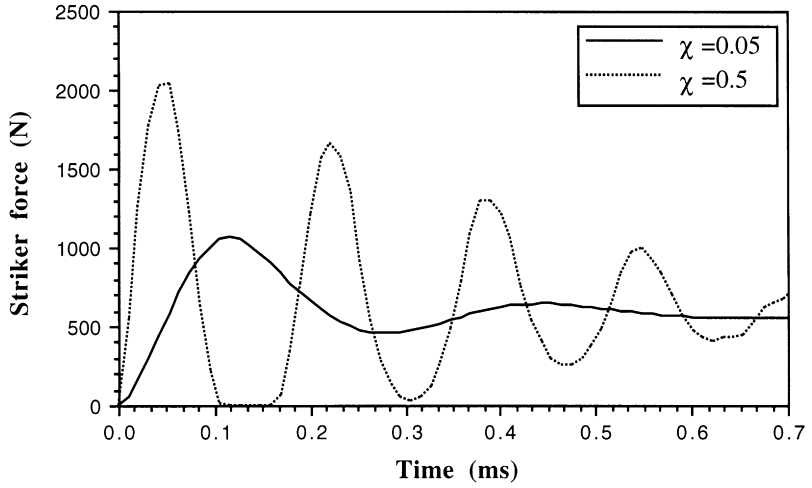

Figure 10 Dependence of predicted load on contact stiffness

model. The same material definition was used to model each sample. The results (*Figure 9*) show an increase in both the frequency and amplitude of the load trace as the overhang length is increased.

The contact stiffness does, however, have a secondary effect (*Figure 10*). Decreasing the contact stiffness reduces both the amplitude and frequency of the striker force oscillations, whilst the mean load remains constant. This result would be expected from a mass-spring model[9].

The load history in the HSDT test is usually measured at the support point at the loaded end of the specimen. Torsional Impedance tests have also been performed by Venizelos[15] using an accelerometer in the striker. Both the applied load at the striker contact point and the reaction

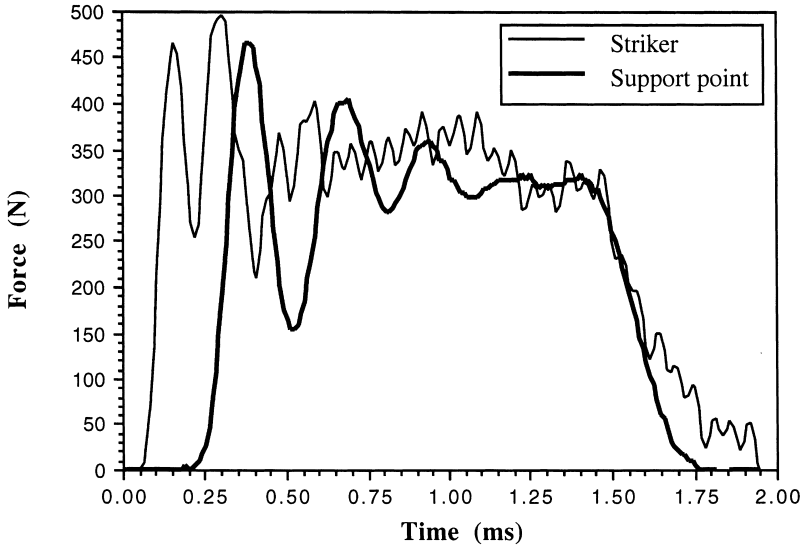

Figure 11 Striker and support loads during the same Torsional Impedance test

force at the support point for one test are shown in *Figure 11*. The load trace from the accelerometer has been considerably smoothed to suppress the 'ringing' of the striker at 13 kHz.

The analysis of the Torsional Impedance test assumes that the striker and support loads are equal: a necessary assumption to reduce the equations of motion to one spatial dimension. Two important facts can be concluded from *Figure 11*:

- The striker initially impacts the specimen significantly earlier than any response can be seen in the support point load.
- The average load, after the initial peak, calculated from the two measurements is the same.

Photographs of high speed torsion deformation taken by Wheel[13] give a further insight into the deformation. A definite initial rotation of the load plane section about an axis close to the centroid can be seen. This rapidly changes to a rotation about the support point.

The above results allow the following conclusions to be drawn about the nature of the deformation close to the load plane. As the striker impacts the specimen, the load plane section begins to rotate about a point close to the centroidal axis and the specimen lifts off the support point. Torsional loading waves emanate from the load plane, in both directions, along the axis of the specimen. The wave travelling towards the impacted free end of the specimen is reflected back towards the load plane as an unloading wave. During this time the rotating sections also gain a small nett downward velocity component due to the continuing downwards motion of the striker.

As the reflected unloading wave reaches the load plane, contact between the specimen and the support point occurs and the reaction force at this point begins to increase, whilst the contact force between the striker and the specimen reduces. This process is repeated, producing the characteristic oscillations in the load trace. The support and striker force oscillations are therefore in anti-phase and the initial increase in support load does *not* correspond to the time of impact but is delayed by approximately one period.

The single-spatial-dimension FD analysis is unable to fully model this deformation, but does account for the contact stiffness and overhang effects. In terms of energy transmission via the torsional wave-guide, the FD analysis should be accurate. The predicted load trace resembles the striker contact force as opposed to the support point load.

CONCLUSIONS

Once effective section shear stress, strain and moduli are defined the Torsional Impedance test provides an ideal method for measuring the effective stress–strain characteristic at the strain rates appropriate to the analysis of the HSDT test. The ultrasonically measured shear modulus is relevant at low shear strains, but at high strains it can over-estimate the shear modulus by a factor of two to three.

Deformation in the Torsional Impedance test is largely controlled by the Saint-Venant wave equation. The dispersive nature of torsional waves in rectangular beams is a secondary effect, which is most apparent in its production of a negative section rotation at the leading edge of the dominant torsional wave.

A finite difference model has been formulated which accurately models the Torsional Impedance test. With some minor adaptations this model can be used to model the HSDT test, as will be presented elsewhere.

REFERENCES

1. Leevers, P. S., *J. de Physique*, 1988, **49**, pC3/231.
2. Wheel, M. A. and Leevers, P. S., *Int. J. Fracture*, 1993, **61**, 331.
3. Gere, J. M., *J. Appl. Mech.* , 1954, **21**, 381.
4. Dioh, N. N., High strain rate behaviour of polymers at various temperatures, PhD thesis, University of London, 1993.
5. Wheel, M. A. and Leevers, P. S., *Int. J. Fracture*, 1993, **61**, 349.
6. Ritchie, S. J. K. and Leevers, P. S., submitted to *J. Strain Analysis.*
7. Ritchie, S. J. K. and Leevers, P. S., submitted to *J. Strain Analysis.*
8. Leevers, P. S. and Williams, J. G., *J. Mat. Sci.* , 1987, **22**, 1097.
9. Williams, J. G., *Int. J. Fracture*, 1987, **33**, 47.
10. Crouch, B., *Computers and Structures*, 1993, **48**, 167.
11. Timoshenko, S. P. and Goodier, J. N., *Theory of Elasticity*, 3rd edn. McGraw-Hill, New York, 1970.

12. Ritchie, S. J. K. and Leevers, P. S., in *Impact and Dynamic Fracture of Polymers and Composites, ESIS 19*, ed. J. G. Williams and A. Pavan. Mechanical Engineering Publications, 1995, p. 137.
13. Wheel, M. A., High speed double torsion testing of pipe grade polyethylenes. PhD thesis, University of London, 1991.
14. Dioh, N. N., Leevers, P. S. and Williams, J. G., *Polymer*, 1993, **34**, 4230.
15. Venizelos, G. P., Investigation of the S4 test for RCP in thermoplastics pipe. PhD Thesis, University of London, 1998.